Understanding the effects of machinability properties of Incoloy 800 superalloy under different processing conditions using artificial intelligence methods

Emine Şap [1], Üsame Ali Usca [2], Serhat Şap [3], Hasan Polat [4], Khaled Giasin[5], Mete Kalyoncu[6]

[1] Department of Electronics and Automation, Vocational School of Technical Sciences, Bingöl University, Bingöl, 12000, Turkey; esap@bingol.edu.tr, https://orcid.org/ 0000-0002-7739-0655
[2] Department of Mechanical Engineering, Faculty of Engineering and Architecture, Bingöl University, Bingöl, 12000, Turkey; ausca@bingol.edu.tr, https://orcid.org/0000-0001-5160-5526
[3] Department of Electricity and Energy, Vocational School of Technical Sciences, Bingöl University, Bingöl, 12000, Turkey; ssap@bingol.edu.tr, https://orcid.org/0000-0001-5177-4952
[4] Department of Electricity and Energy, Vocational School of Technical Sciences, Bingöl University, Bingöl, 12000, Turkey; hasanpolat@bingol.edu.tr, https://orcid.org/ 0000-0001-5535-4832
[5] School of Mechanical and Design Engineering, University of Portsmouth, Portsmouth, PO1 3DJ, UK; khaled.giasin@port.ac.uk, https://orcid.org/0000-0002-3992-8602
[6] Department of Mechanical Engineering, Faculty of Engineering and Natural Sciences, Konya Technical University, Konya, 42000, Turkey; mkalyoncu@ktun.edu.tr, https://orcid.org/0000-0002-2214-7631

*Corresponding author: esap@bingol.edu.tr (E.Ş), ausca@bingol.edu.tr (Ü.A.U.), ssap@bingol.edu.tr (S.Ş.), khaled.giasin@port.ac.uk (K.G.)

Abstract: Incoloy 800 is frequently used in high-temperature applications as it has the ability to retain good metallurgical stability at elevated temperatures. Due to the nature of the applications used for, parts made from Incoloy 800 usually require different machining processes such as milling and turning. Therefore, the current study aims to investigate the milling performance of Incoloy 800 under different cutting parameters (75-150 m/min and 0.075-0.15 mm/rev) and cooling conditions namely dry, flood, Minimum Quantity Lubrication (MQL) and Cryogenic (Cryo)+MQL. It was observed that all machinability metrics improved in the MQL+Cryo C/L environment. It is noticeable that the surface roughness value improved by 30% in this environment. In addition, a model based on artificial neural networks (ANN) and particle swarm optimization (PSO) was proposed to analyze the

results and predict optimum cutting parameters. It appears that Cryo+MQL strategies are the best option for all cutting parameters. It was found that the estimations for surface roughness, flank wear, and cutting temperature with the proposed ANN architecture are achieved with overall relative error of 6.08%, 12.38%, and 8.32%, respectively. The proposed model resulted in good performance between the experimental test data and the predicted values. The developed model made the most efficient predictions for the MQL+Cryo cutting environment. It was observed that the estimations of the different input parameters in the MQL+Cryo cutting environment present a relative error of 8.36%, 1.46%, and 2.38% for surface roughness, flank wear, and cutting temperature, respectively. By utilizing the predictive capability of the trained ANN model, the optimization of the input parameters was carried out with the PSO technique. Thus, with the developed PSO-ANN model, promising findings were obtained in overcoming important handicaps such as time and cost in experimental studies.

Keywords: Incoloy 800; Hybrid cooling; Artificial intelligent; Machining; MQL; LN_2

Nomenclature

MQL	Minimum Quantity Lubrication
LN_2	Liquid Nitrogen
ANN	Artificial Neural Network
PSO	Particle Swarm Optimization
C/L	Cooling/Lubricating
V_c	Cutting Speed
f	Feed Rate
R_a	Average Surface Roughness
T_c	Cutting Temperature
V_B	Flank Wear

1. Introduction

Incoloy 800, also known as Inconel alloy 800, is a heat resistant alloy used in engineering applications at a wide range of temperatures ranging from -200 to +815 °C

[1]. It is mainly used in heat treatment and high-temperature industrial applications such as ovens, heat exchangers and energy power plants. Since these nickel-based superalloys have low heat transfer coefficients and high satiety conditions, some difficulties arise in their process [2, 3]. Incoloy 800 is a complex material, and a developing processing index requires significant research. The correct determination of cutting tools, cutting parameters, cooling/lubrication (C/L) condition, and the right decision of processing strategies play significant roles in the machinability of superalloys [4]. For example, coated cemented carbide cutting tools are preferred due to the high hardness of superalloys, especially that those alloys are usually machined at higher cutting speeds. This phenomenon also results in elevated cutting temperatures at the interface between the cutting tool and the workpiece [5]. Nevertheless, the tools used in machining super alloys are susceptible to thermal cracks and rapid tool wear which adversely affect the part surface finish. This has additionally prompted scholars to explore the impact of C/L technologies on both the resultant surface finish and tool wear [6]. Although dry cutting is considered environmentally friendly, it is well-known that it is not practical for machining superalloys. In addition, some studies have confirmed this by emphasizing that the machinability of super alloys is reduced under dry conditions [7-10]. The utilization of cutting fluids stands out as one of the prevalent approaches to enhance machinability indices [11, 12]. Cutting fluids play a crucial role in chip evacuation and mitigating heat generation within the cutting zone by diminishing friction between the workpiece and the cutting tool [13-15]. However, the use of cutting fluids, especially petroleum-based conventional cutting fluids, with the traditional method have health and environmental implications which adds extra costs to the manufacturing process [16]. An alternative is to use smaller amounts of coolants via a technology called minimum quantity lubrication (MQL). With this method, environmentally friendly vegetable-based oils can be used [17]. MQL uses air mixed with a minimal volume of oil that forms a spray focused on the cutting zone. Hence, the oil establishes a thin film within the cutting zone, thereby diminishing friction between the workpiece and the cutting

3

tool [18, 19]. Previous studies reported that MQL method directly improves the machinability metrics [20-24]. Despite all this, it was emphasized that the MQL might not be efficient when used in extreme machining environments (high speed machining, machining of difficult to cut alloys) [5]. An additional option involves the adoption of sustainable and environmentally friendly cryogenic cooling, a subject that has garnered increased attention from researchers in recent times. Chetan et al. [25] reported that cryogenic cooling reduces tool wear by 0.2 mm. Deshpande et al. [26] stated that cutting tool life and workpiece surface quality improved when using cryogenic cooling conditions. Similarly, it was reported that cryogenic cooling reduces tool wear and cutting temperatures, and has a good effect on chip morphology [27-29]. Chen et al. [30] reported that providing the hybrid cryo-MQL condition achieved twice the tool life by minimizing the friction coefficient compared to dry machining. In this technique, it was reported that the cryogenic coolant provides effective cooling, while using MQL improved tribological conditions [31, 32]. Nowadays, the optimization of machining parameters and the machined part quality are of great importance that aims to save costs and increase productivity [33]. Accurate determination of cutting parameters shortens the processing time and reduces material loss and energy consumption. In machining, AI (artificial intelligence) often emerges as a technology that can be used to determine optimal cutting parameters. Artificial intelligence algorithms scrutinize the characteristics of materials, tools, and machinery to ascertain optimal cutting parameters for the machining process, thereby contributing to the enhancement of the final part quality. Artificial neural networks (ANN) is a concept produced by mathematical modeling of biological neural networks [34]. ANN mathematically mimics the behavior and learning skills of brain nerve cells [35]. It is actively used in the solution and optimization of complex problems with a large number of trainable parameters in its structure [36]. It uses a transfer function that produces outputs corresponding to the input parameters, depending on a weighting factor adapted during training [37]. Its exceptional ability to learn complex and nonlinear connections has made it popular for estimation and optimization models of

input-output parameters [36, 38-40]. The connections between input cutting parameters and outputs, such as surface roughness, flank wear, and cutting temperature, can be mathematically modeled using the ANN approach. Thus, efficient and robust simulations can be performed before a real-time application.

In material processing, optimum machining performance in cutting tool life, time, and cost can be achieved by modeling the relationship between input parameters and outputs [41]. However, selecting an appropriate heuristic optimization model is required to apply the optimum input parameters to the ANN input. Thus, the ANN-based optimal cost function can be obtained. Numerous optimization techniques inspired by nature were proposed recently [42]. In this context, genetic algorithm (GA) [43], particle swarm optimization (PSO) [44], ant colony optimization (ACO) [45] and artificial bee colony (ABC) [46] are among the most frequently used optimization models. Compared to other optimization techniques, the PSO technique stands out in terms of containing few parameters to adjust, the memory ability of herd members, and preserving herd diversity [47]. Therefore, it was frequently preferred in the literature for parameter optimization in material machinability [48-52]. With this motivation, this study proposes a PSO-based ANN (PSO-ANN) approach to determine the optimum machining parameters and most suitable cooling technology.

The number of studies on the machinability of Incoloy 800 in the literature is limited. At the same time, the machinability and power consumption properties of superalloys, which have an important place in the industry, were investigated using different sustainable cooling techniques. In particular, the lack of optimal cutting parameters will lead to significant energy, time, and cost losses. Therefore, the current study aims to investigate the machinability of Incoloy 800 by combining AI algorithms and cooling technologies to improve the machining process.

2. Materials and methods

2.1. Workpiece and experimental procedure

The milling tests were conducted on a Ø50 mm and 15 mm Incoloy 800 material consisting of nickel-based iron. It is known that this material has high corrosion resistance, high-temperature resistance, and high creep rupture resistance [53, 54]. Chemical composition and mechanical properties of Incoloy 800 are presented in Tables 1 and 2, respectively.

Table 1. Chemical composition of Incoloy 800

Elements	Fe	Ni	Cr	Mn	Si	Cu	Al	Ti	C	S
Rate	39.5% min	30% min	19% min	1.5% max	1% max	0.75% max	0.15% min	0.15% min	0.1% max	0.1% max

Table 2. Mechanical properties of Incoloy 800

Property	Metric
Density	7.94 g/cm³
Thermal conductivity	11.5 W/m.°C
Electrical resistivity	0.989 μΩ.m
Tensile strength	600 MPa
Yield strength	275 MPa
Hardness	184 HB

The experimental procedures were conducted utilizing a Dahlih MCV 860 three-axis (x-y-z) CNC milling machine, featuring a maximum rotational speed of 10,000 rpm and a power rating of 7.5 kW. In the experiments, the single-edged face milling cutter with a diameter of 12 mm and Al-TiN coated insert (HM90 APKT1003 PDR-HM IC908, Iscar) were used. Two cutting speeds (75-150 m/min) and two feed rates (0.075-0.15 mm/rev) were used. Preliminary experiments were effective in the selection of the aforementioned cutting parameters. A depth of cut of 1 mm and a cutting width of 12 mm were chosen during the milling tests. The milling experiments were conducted employing the Zig tool path and employing a down-milling approach. In addition, four different C/L conditions were used throughout the experiments. Table 3 shows the input factors and their levels which were used in the milling tests. The full experimental design was determined for the milling tests, and a total of 16 experiments were carried out.

6

Table 3. Levels and factors of experimental parameters

Parameters	Unit	Level 1	Level 2	Level 3	Level 4
C/L conditions	-	Dry	Flood	MQL	Cryo+MQL
Cutting speed	m/min	75	150	-	-
Feed rate	mm/rev	0.075	0.15	-	-
Depth of cut	mm	1	-	-	-
Width of cut	mm	12			

2.2. Cooling methods setup

Machinability tests were carried out under four different C/L conditions. Mineral-based metalworking fluid is preferred under flooding conditions. The working fluid is formed by adding 8% mineral oil to pure water. For the MQL C/L environment, an MQL system from Kar-Tes (Turkiye) and a Werte branded oil with KT-2000 hydrodynamic lubrication was used. In the MQL system, a nozzle having a diameter of 3 mm was employed, with the distance from the nozzle to the workpiece set at 100 mm. The MQL system pressure was configured at 6 bar, and the lubrication flow was established at 50 mL/h. As for the cryogenic cooling environment in the MQL+Cryo hybrid C/L condition, liquid nitrogen (LN_2) sourced from a self-pressurized tank at -196 °C was utilized. For LN_2, the system pressure and flow rate were set to 6 bar and approximately 30 L/h, respectively. The liquid nitrogen hose incorporated a nozzle with a fixed diameter of 5 mm, positioned at a distance of 100 mm from the workpiece. The final C/L condition was made by using LN_2 and MQL cooling techniques simultaneously to form a hybrid cooling method and assess their impact when used together during the milling process. The experiment scheme is seen in Figure 1.
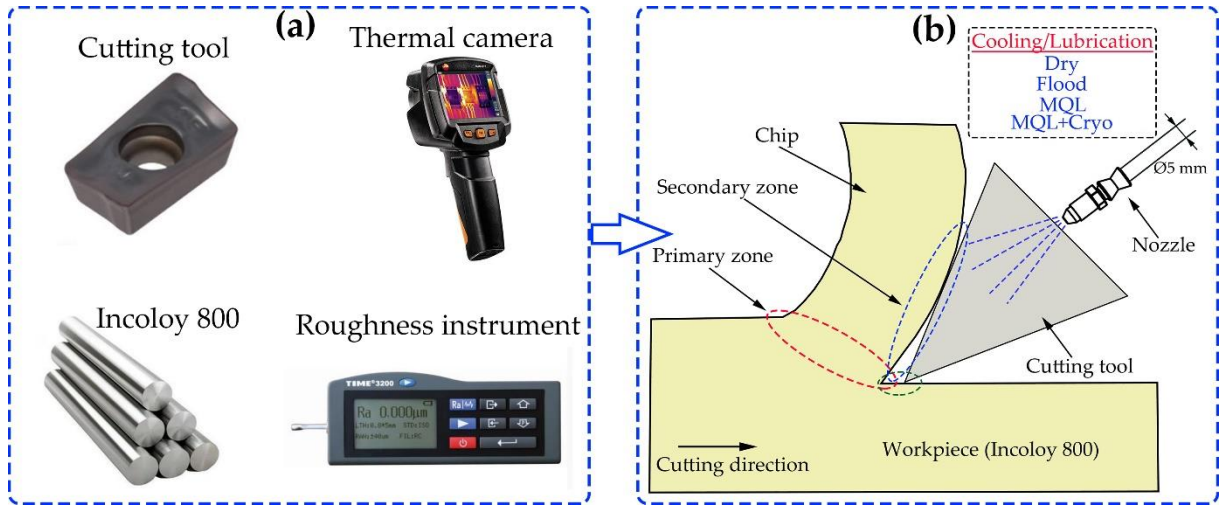
Figure 1. Experiment scheme showing (a) material and equipment used in the milling tests (b) an illustration of the milling test setup

2.3. Post-machining analysis

To determine the machinability characteristics of the Incoloy 800 workpiece, a series of post-machining tests were conducted to evaluate the quality of the machined parts. The average surface roughness (R_a) of the machined components was assessed using a TIME 3200 surface roughness measurement device. Surface roughness measurements were conducted at five distinct locations on the machined surfaces for each specimen. The largest and smallest values were subtracted, and the mean of the remaining values was computed. The temperature within the cutting zone was monitored utilizing a Testo 871 infrared thermal camera with a resolution of 240x180 pixels. The reported cutting temperature measurements were obtained approximately 500 mm away from the contact region between the cutting tool and the workpiece. The maximum flank wear of the cutting tools was measured using Insize ISM-PM200SB digital measuring microscope. In our current study, temperatures were measured in the machining zone with a thermal camera. The measurement was taken just before the processing was completed. Since coolants are generally transferred to the cutting area in a pulverized manner, the cutting fluids around do not affect the measurement.

2.4. Artificial Neural Network

ANN is a mathematical imitation inspired by the behavior and learning abilities of the biological nervous system. By a trained ANN model, the patterns not previously presented to the network can be classified, and an estimation of the patterns can be made [35]. An ANN structure generally consists of an input layer with many neurons, one or more hidden layers, and an output layer [40]. Throughout the network, each layer processes the information from the previous layer and transmits it to the next layer. Input data is given to the hidden layer with trainable weights [34]. The weight and bias parameters connecting the input layer to the subsequent hidden layer are initially assigned random values. Subsequently, the activation of each hidden neuron is computed based on the outputs of the input units and the corresponding weights linking the input and hidden units [55]. While the neurons in the input layer (x_i) transmit the input information to the neurons in the hidden layer (j), the input information of the neurons in the hidden layer (w_{ij}) is multiplied by their weights and collected with bias (b_j) [35]. Thus, the output of an ANN model (y_j) can be represented as follows.

$$y_j = f(\sum_{i=0}^{d^{l-1}}(w_{ij}^l x_i^{l-1} + b_j)) \tag{1}$$

Here, f represents the activation function, d represents the network size, and l represents the number of layers. This study's input layer; consists of three neurons representing cutting speed, feed rate, and coolant type. Furthermore, three distinct output layers were taken into account, specifically addressing surface roughness, flank wear, and cutting temperature. It is important to note that there exists no standardized guideline for determining the number of neurons in the hidden layer [40]. It is usually determined by trial and error, depending on the complexity of the dataset [36]. According to the complexity of the data set used in this study, using a hidden layer was appropriate. The number of neurons in the hidden layer was evaluated gradually,

starting from 1 to 100. Optimum ANN architecture was determined by considering error and analysis time. Figure 2 shows the proposed ANN structure in the study.
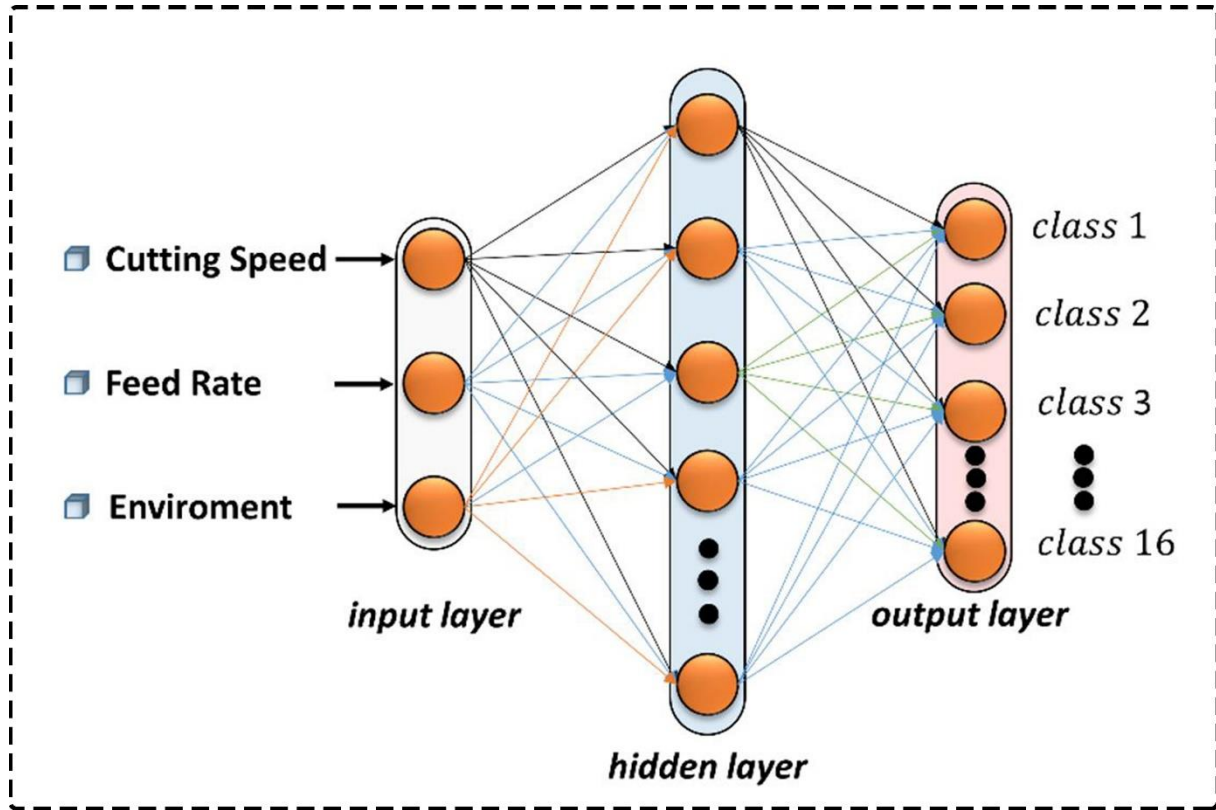

Figure 2. The proposed ANN structure for prediction

The average terrestrial error targeted during the training phase was set to 0.001, and the number of iterations to 1000. The learning rate was determined as 0.7. The activation functions employed were the hyperbolic tangent sigmoid (tansig) and the logarithmic sigmoid (logsig) functions, respectively. Levenberg-Marquardt (trainlm), scaled conjugate gradient (trainscg), and gradient with momentum (traingdm) training algorithms were evaluated to ensure the optimum performance of the backpropagation algorithm. Trainscq showed the best training performance.

2.5. Particle swarm optimization

Particle Swarm Optimization (PSO) is characterized as a stochastic optimization technique based on population dynamics [44]. The cooperative behavior of populations, such as flocks of birds and fish, inspires the proposed optimization algorithm [42, 52]. Because the PSO technique is simple, offers superior convergence,

and high accuracy, it is suitable for multivariate and complex problems. [52, 56]. The positions of each particle (swarm member) within the PSO record possible solutions to the optimization problem. Following each iteration, the position of each particle undergoes an update based on its individual best position (pbest) and the collective best position within the swarm (gbest) [42]. Thus, after the PSO is started with a group of random particles, it is tried to determine the optimum depending on the positions and velocities of all particles [47]. After finding the pbest and gbest regarding the positions of the particles, each particle's velocity and position are updated by applying the following equations.

$$v_{ij}(t + 1) = w.v_{ij}(t) + c_1 r_1 \left(pbest_{ij}(t) - x_{ij}(t)\right) + c_2 r_2 \left(gbest_{ij}(t) - x_{ij}(t)\right) \qquad (2)$$

$$x_{ij}(t + 1) = x_{ij}(t) + v_{ij}(t + 1) \qquad (3)$$

Here $j = 1, 2, 3, \dots n$, v_{ij} j. in iteration i. represents the particle's speed. x_{ij} is j. in iteration i. represents the current of the particle. r_1 and r_2 are random numbers, and c_1 and c_2 are learning coefficients. For a better understanding of the step-by-step operation of the PSO algorithm, the block diagram of the relevant process flux in the PSO algorithm is shown in Figure 3.
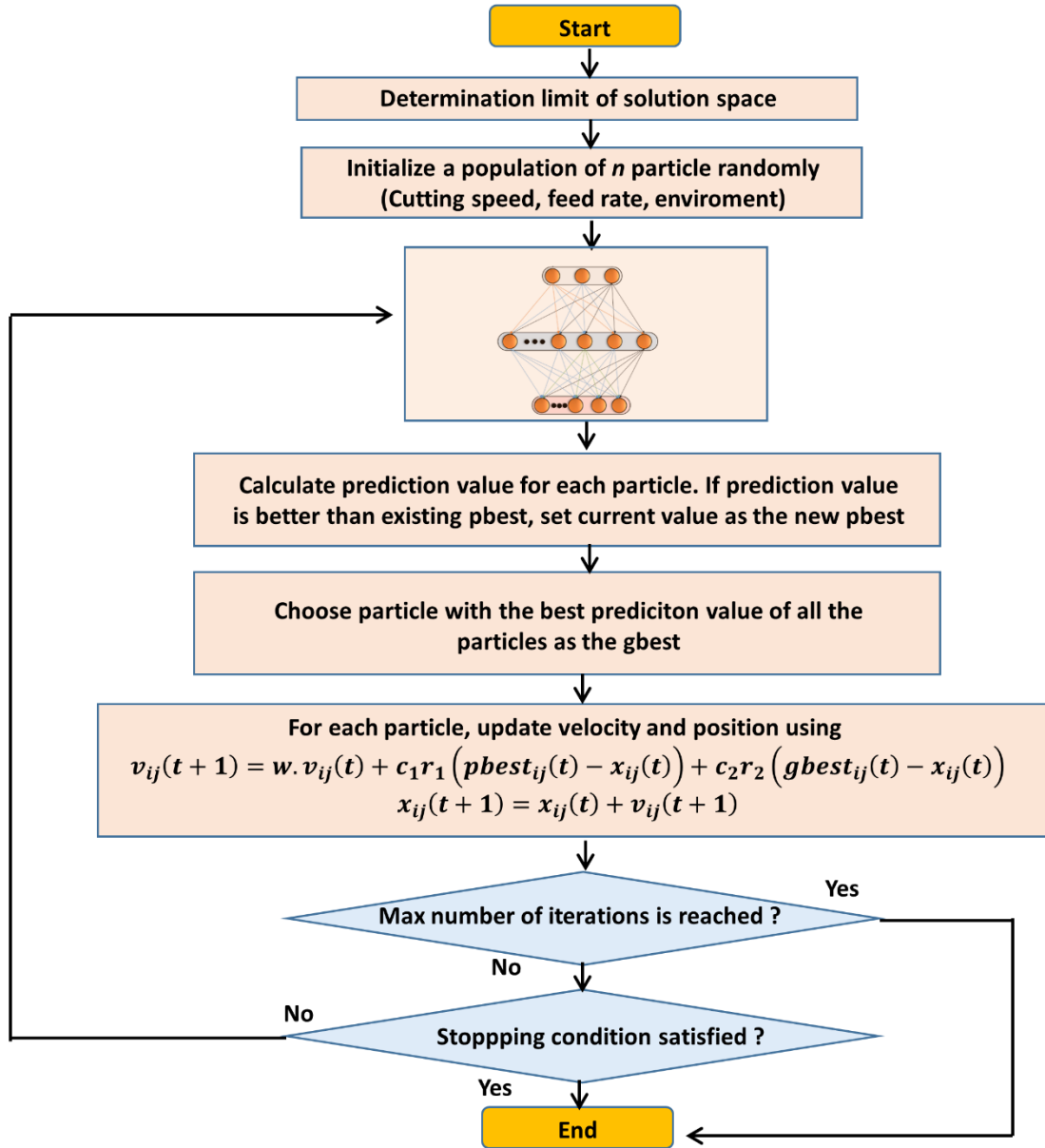
Figure 3. The flow chart of the proposed PSO algorithm

3. Result and discussion

3.1. Surface roughness analysis

Figure 4 illustrates the surface roughness obtained by varying cutting speed and feed rate under different cooling conditions. The findings indicate that the concurrent application of liquid nitrogen (LN2) and Minimum Quantity Lubrication (MQL) can result in a substantial reduction of surface roughness, reaching up to 400%. This improvement can be attributed to the synergistic effects of the two cooling techniques, where MQL enhances surface lubrication between the cutting tool and the workpiece,

12

while LN₂ mitigates cutting temperatures within the cutting zone. Previous studies have reported an association between elevated temperatures during the machining of nickel-based superalloys and increased surface roughness [57]. The outcomes further indicated that surface roughness is relatively insensitive to variations in both cutting speed and feed rate. Nevertheless, a discernible decrease in average surface roughness was observed with an increase in cutting speed, a phenomenon attributed to the concurrent rise in temperature. As the cutting temperature increases, the machining area softens and can reduce BUE formation on the cutting tool. Thus, a higher quality surface can be obtained [58]. The existing body of literature provides corroborative evidence for this circumstance [59, 60]. Simultaneously, it is evident that augmenting the feed rate resulted in an escalation of surface roughness, whereas the impact of increasing cutting speed appeared to be comparatively less pronounced.
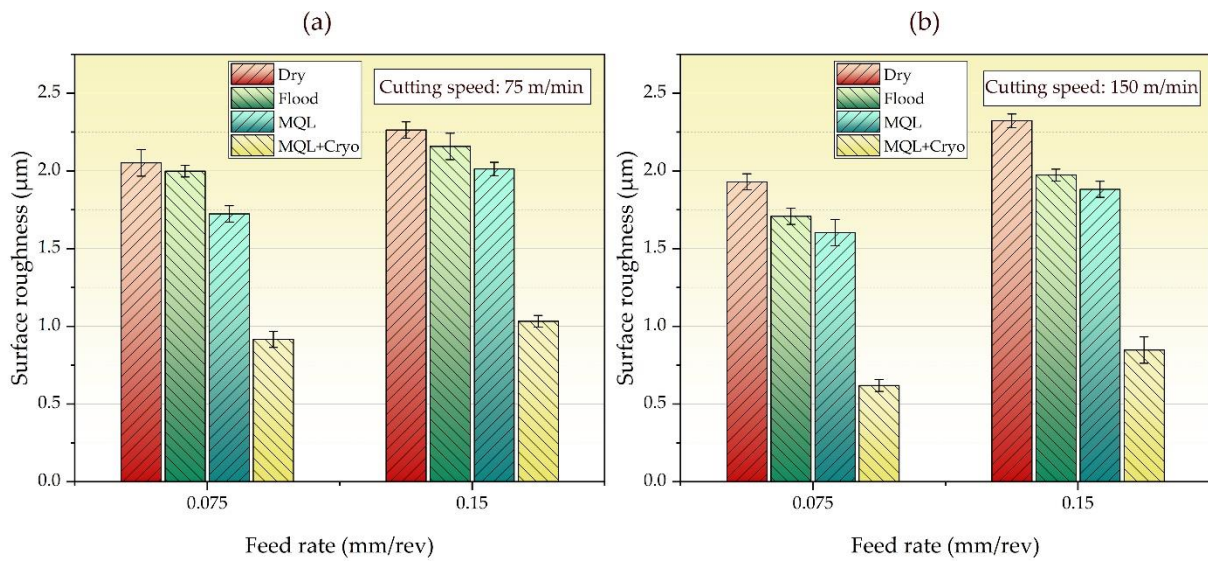

Figure 4. Effects of different C/L condition on surface roughness; a) 75 m/min, b) 150 m/min

Figure 5 presents the 2D and 3D surface topographies of machined specimens subjected to various cutting environments. Notably, the dry-cutting environment exhibited the most prominent peaks and valleys. The resulting average Ra values were 1.929 μm, 1.708 μm, 1.603 μm, and 0.619 μm for dry, flood, Minimum Quantity Lubrication (MQL), and MQL combined with cryogenic (MQL+Cryo) cutting

conditions, respectively. Using the MQL+Cryo cooling strategy, cooling and lubrication are performed simultaneously, reducing the surface roughness significantly. The observed trend indicates a reduction in both peaks and valleys as the transition is made from the dry cutting environment to the MQL+Cryo cutting environment. During lubrication with MQL, a hydrodynamic film is formed. This mitigates the frictional forces between the tool and the workpiece. Moreover, the combined application of LN_2 and MQL contributes to a reduction in cutting tool wear by moderating the temperature within the cutting zone. As a result, the longevity of the cutting tool's effective performance is extended, thereby enhancing surface quality [58].
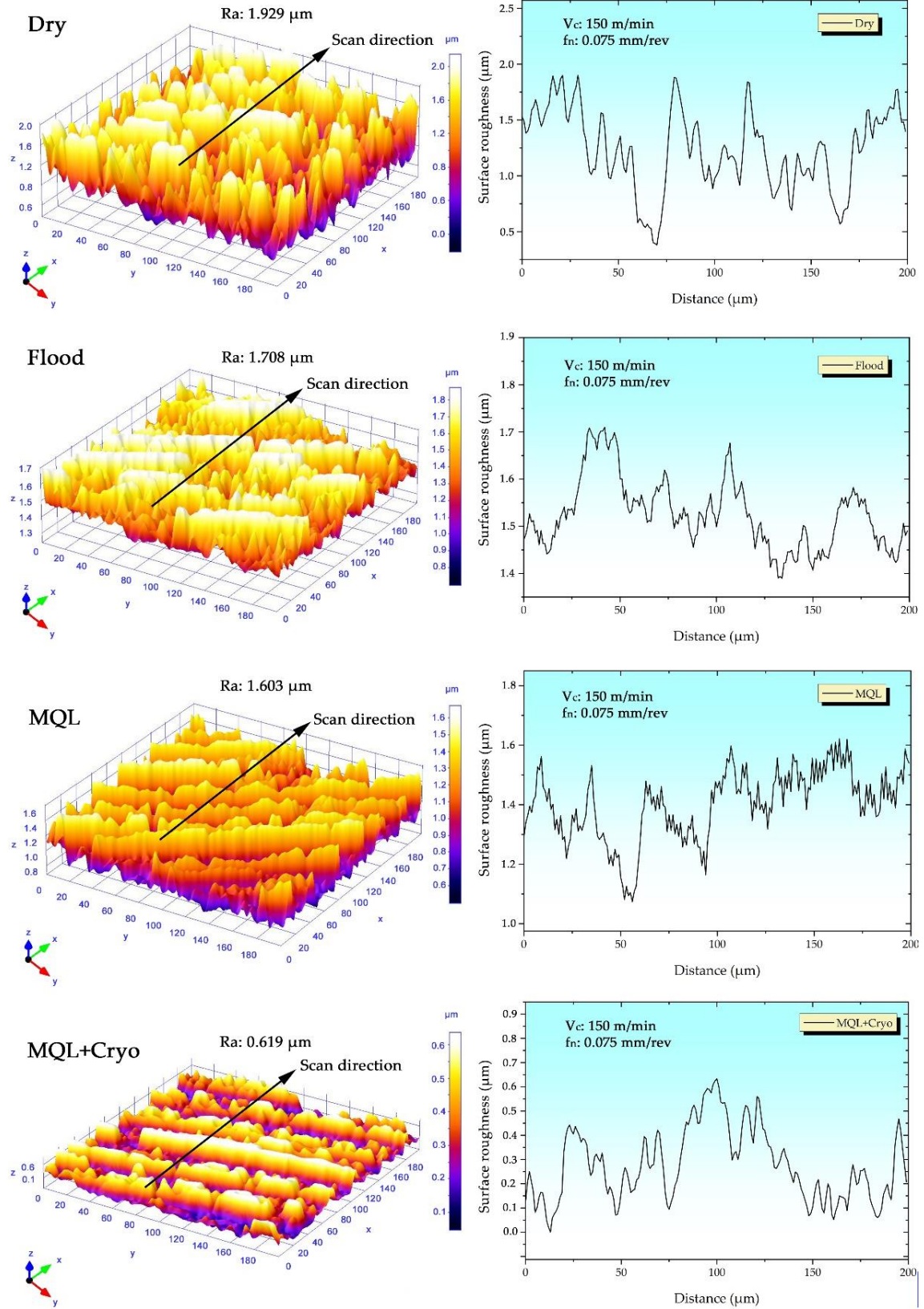
Figure 5. 3D and 2D surface topographies of samples milled in different cutting environments

3.2. Flank wear analysis

Figure 6 illustrates the measurement of flank wear during the machining process across various cutting environments. Generally, it is evident that the utilization of coolants contributes to the reduction of flank wear. The minimum flank wear, measuring at 0.415 mm, was observed in the MQL+Cryo environment. It was determined that flank wear exhibited an increase with cutting speed, ranging from 75 m/min to 150 m/min. Conversely, an increase in feed rate resulted in a reduction in flank wear. Elevated cutting speeds contribute to heightened temperatures at the interface between the cutting tool and the workpiece, leading to an accelerated rate of tool wear [61]. It was observed that the cooling effect for flank wear decreases at high cutting speeds. The reduction of the cooling factor effect at high speeds in milling operations is generally dependent on thermal and kinematic factors. The thermal impact arises from the heat generated by the friction between the cutting tool and the workpiece, and its rapid dissipation becomes challenging, particularly at elevated cutting speeds. The kinematic effect is due to the rapid movement of the cutting edge, which can shorten the time for the coolant to intervene. Other factors that can affect the effectiveness of the coolant can include cooling unevenness and mist formation. Thus, it was observed that there is not much difference in flank wear values.
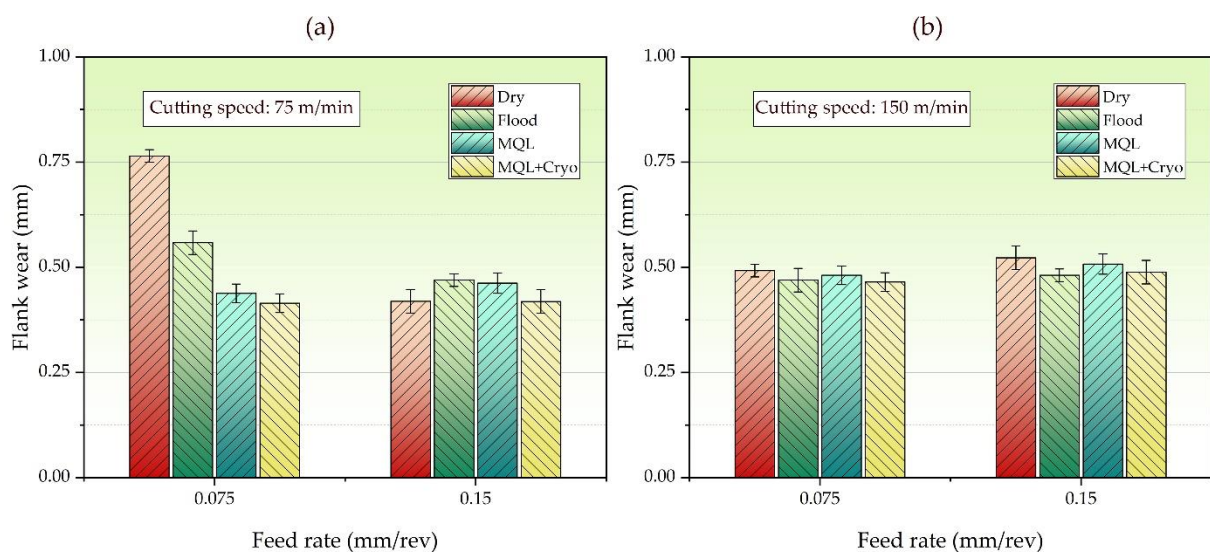

Figure 6. Effects of different C/L condition on flank wear; a) 75 m/min, b) 150 m/min

16

Figure 7 depicts SEM images of inserts employed under diverse cutting environments. Within these SEM images, regions indicative of flank wear and notch wear are demarcated along the edges of the cutting tool. In the flood environment, the edge and nose of the insert are subjected to thermo-mechanical loading. This results in edge chipping and nose wear [62]. EDS images are given in Figure 8, and mapping analysis images in Figure 9. The most notable phenomena from the SEM images are that the size of the worn area in the tool is smaller when using Flood, MQL and MQL+LN$_2$. It can be seen that the wear zone is smaller, especially in MQL+LN$_2$ conditions. This shows that these methods, which provide more effective cooling, reduce tool wear by lowering the temperature generated during cutting.

Chipping can be seen to occur under dry, MQL and MQL+LN$_2$ and to a much lesser extent under flood conditions. This could be due to the when the cutting tool is subjected to excessive wear, particle detachment (chipping) on the surface or edges of the material of the cutting tool often occurs as a result of the wear process. There may be various mechanisms behind this phenomenon: the most important of which is mechanical fatigue. The edges of the cutting tool can be subjected to fatigue stress during repetitive cutting movements. This stress can cause microcracks to form in the material of the cutting edge and eventually lead to chip breakage.
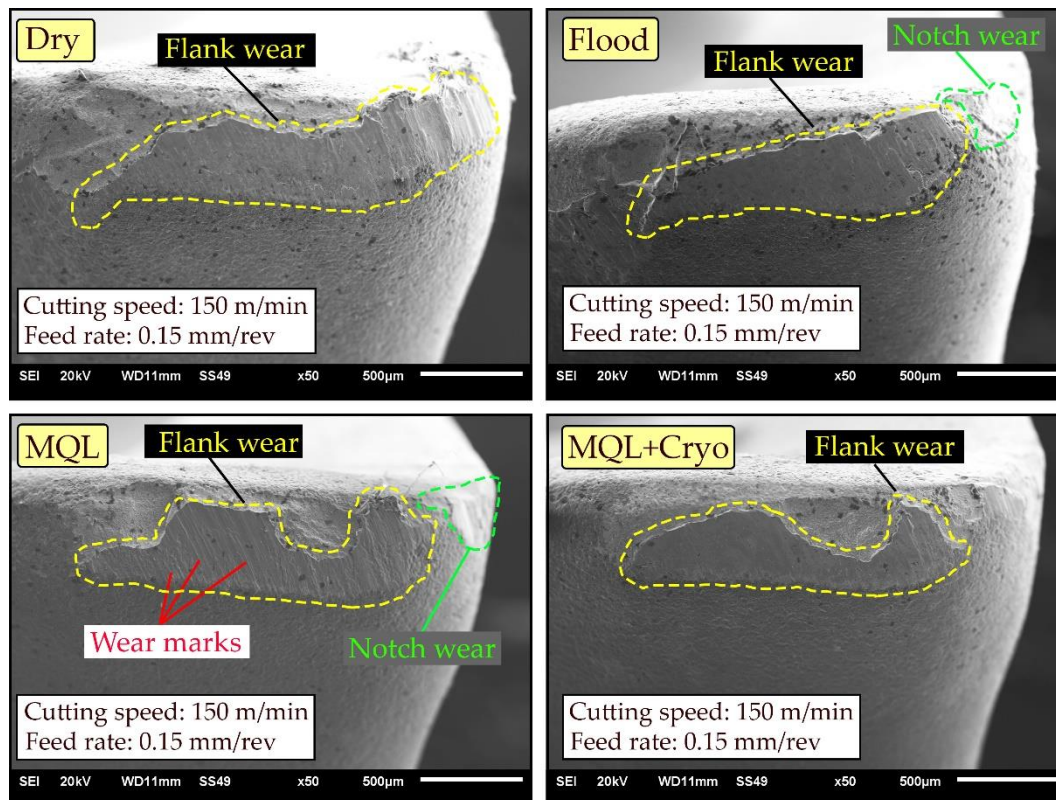
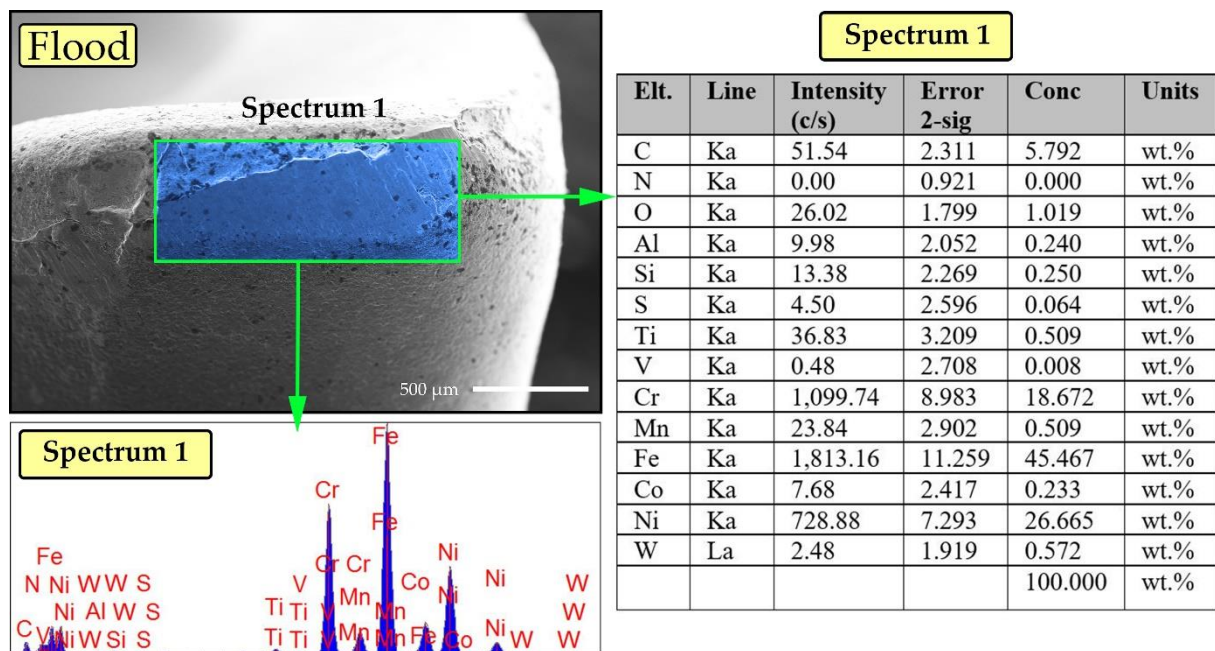**Figure 7.** SEM images of inserts used in different cutting environments

Elt.	Line	Intensity (c/s)	Error 2-sig	Conc	Units
C	Ka	51.54	2.311	5.792	wt.%
N	Ka	0.00	0.921	0.000	wt.%
O	Ka	26.02	1.799	1.019	wt.%
Al	Ka	9.98	2.052	0.240	wt.%
Si	Ka	13.38	2.269	0.250	wt.%
S	Ka	4.50	2.596	0.064	wt.%
Ti	Ka	36.83	3.209	0.509	wt.%
V	Ka	0.48	2.708	0.008	wt.%
Cr	Ka	1,099.74	8.983	18.672	wt.%
Mn	Ka	23.84	2.902	0.509	wt.%
Fe	Ka	1,813.16	11.259	45.467	wt.%
Co	Ka	7.68	2.417	0.233	wt.%
Ni	Ka	728.88	7.293	26.665	wt.%
W	La	2.48	1.919	0.572	wt.%
				100.000	wt.%

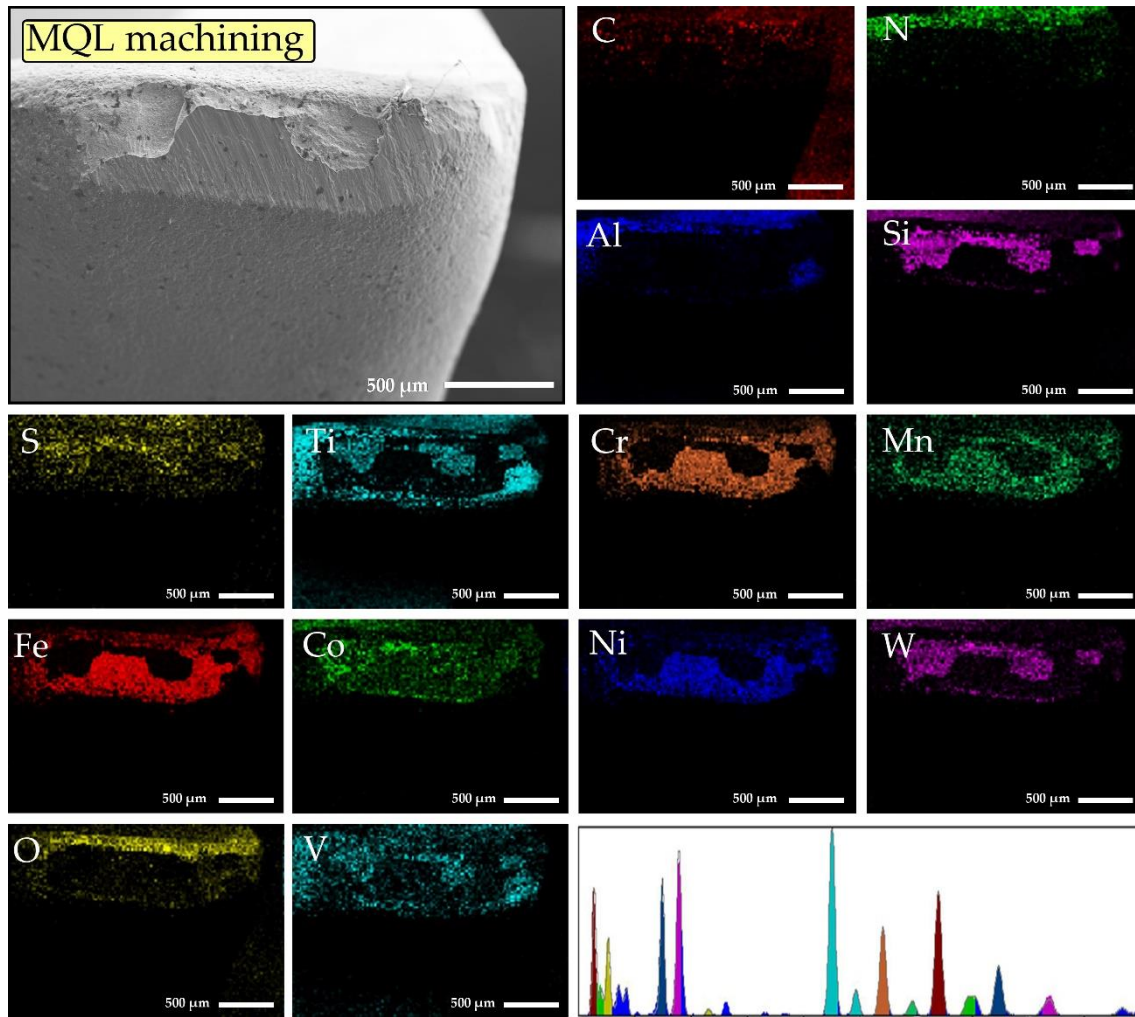**Figure 8.** EDS analysis of insert used in a flood machining environment

Figure 9. Mapping analysis of the insert used in the MQL environment

3.3. Cutting temperature analysis

Figure 10 illustrates the maximum cutting temperature recorded at the cutting zone across distinct cutting environments. The peak cutting temperature, reaching 317 °C, was observed in the dry cutting condition. Similar results also confirms that machining under dry condition usually yields highest temperatures compared to those generated when using coolants [63, 64]. The minimum cutting temperature, recorded at 45 °C, was achieved within the MQL+Cryo environment, employing a cutting speed of 75 m/min and a feed rate of 0.075 mm/rev. The combined effect of lubrication and cooling provide maximum efficiency in reducing the cutting temperatures at the cutting zone and carrying away some of the heat. It be also seen that applying MQL alone doesn't provide sufficient reduction of temperature at the cutting zone. This is mainly due to

the fact that MQL is intended to be used as a lubricant rather than a coolant to remove heat. Most of the lubricant from MQL evaporates once the machining process is complete leaving no signs of lubrication behind. The flood coolant and MQL+LN$_2$ are both more efficient in taking away large amounts of the heat generated at the cutting zone. In particular, it was determined that MQL+LN$_2$ provides effective cooling/lubrication at high and low cutting parameters. In a study, it was emphasized that MQL+LN$_2$ creates an effective cooling/lubrication environment [27].
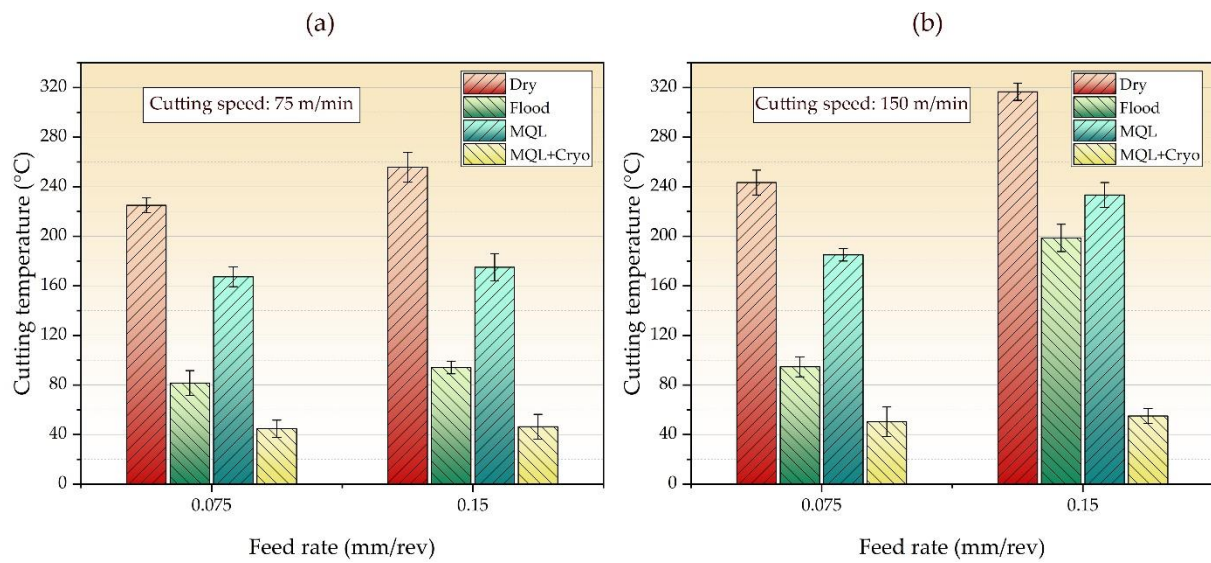

Figure 10. Effects of different C/L condition on cutting temperature; a) 75 m/min, b) 150 m/min

3.4. Chip morphology

Figure 11 depicts the impacts of various cooling and lubrication techniques on the process of chip formation. It is observed that, within a dry environment, the size of the chip diminishes progressively as the system transitions towards the MQL+Cryo environment. This is due to improved chip breakability caused by the increased plasticity of the uncut chip. Serrations are discernible along the edges of chips produced under dry, flood, and MQL conditions. In contrast, chips obtained within the MQL+Cryo environment exhibit reduced instances of serrations.
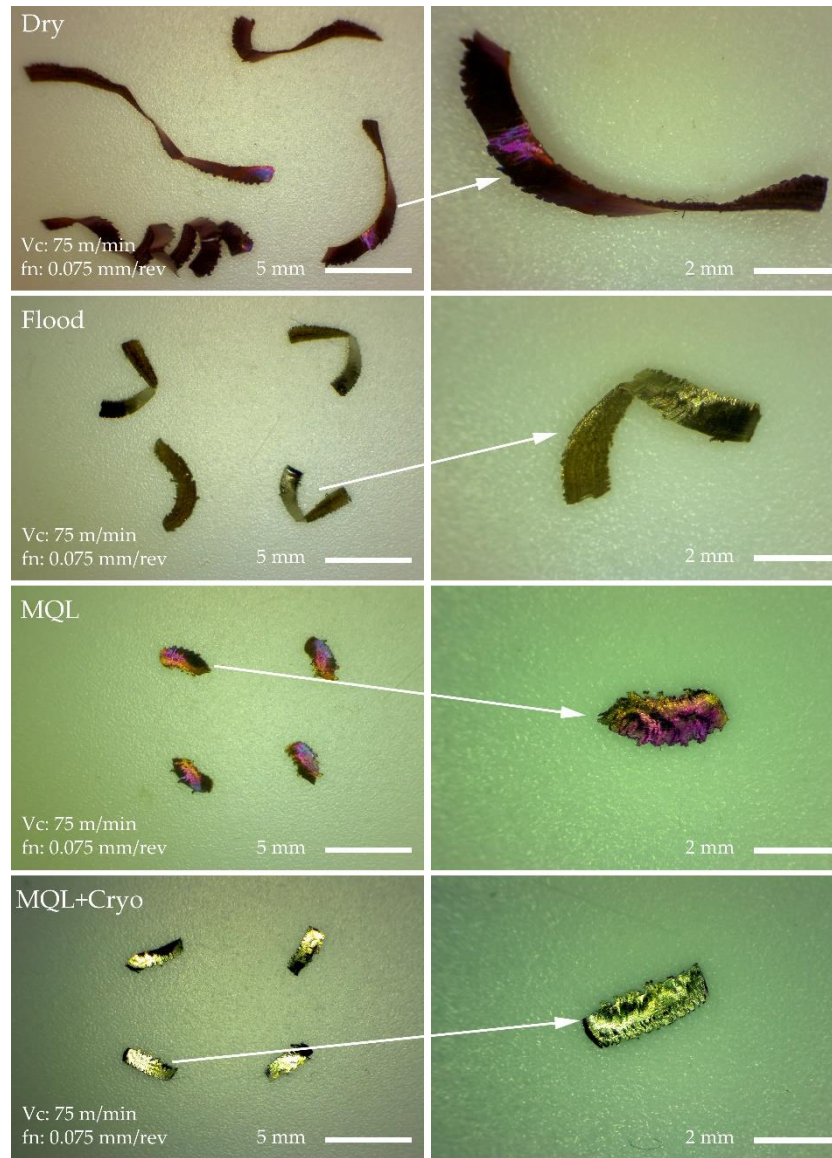
Figure 11. Chip images obtained in different cutting environments

The main reason why serrated chips are undesirable is that it makes the machining process difficult to control, reduces the machined surface quality and accelerates the wear of the cutting tool. Therefore, it is important to use appropriate cutter geometry, cutting parameters and cooling methods to ensure smooth and uninterrupted chip formation during the milling process. It can be said that the appropriate C/L condition for producing acceptable chips for this study is MQL+LN$_2$. This is supported by a study in the literature [58].

3.5. Artificial intelligence analysis

In this study, the proposed PSO-ANN model was developed in Matlab to estimate the outputs corresponding to the milling parameters and to determine the optimum parameters. The determination of the appropriate number of neurons in the hidden layer for the ANN model, constituting the fundamental framework of the proposed model, was achieved through iterative experimentation. Regarding the number of neurons in the hidden layer, different ANN models were tested separately each time, and the final structure with the best performance was determined.
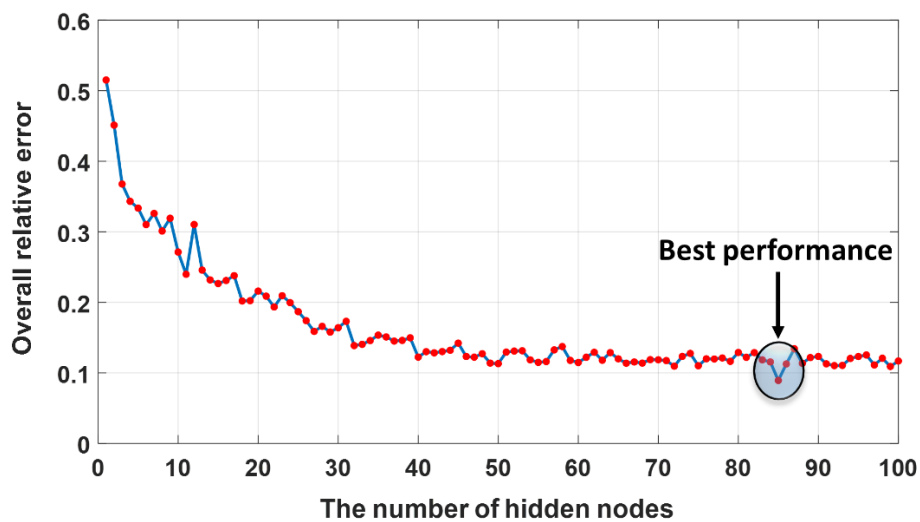

Figure 12. RE performance distribution in prediction with the number of neurons

As seen in Figure 12, the estimation performance increased with the number of neurons in the hidden layer. The lowest RE value was obtained as 0.0893 for 85 neurons. Therefore, an architecture of a 3×85×16 structure was used in this study. The estimation results obtained with the proposed architecture are shown in Table 4. For the training of the network, 16 milling experiments with three different cutting parameters were used. In order to evaluate the performance of the proposed ANN-based prediction model, 10 milling experiments consisting of different cutting parameters that were not previously shown to the network were used as test data.

Table 4. Evaluation of prediction performance in terms of relative error (re) for experimental test data

Inputs			Outputs						
			Surf. Roughness (µm)		Flank wear (mm)		Cutt Temp (°C)		%
Cutting Speed	Feed Rate	Environment	Exp.	Predict	Exp.	Predict	Exp.	Predict	Overall (re)
75	0.1	Dry	2.198	2.204	0.625	0.462	235	213.25	11.81
100	0.1	Dry	2.125	2.183	0.702	0.492	248	243.77	11.40
150	0.1	Dry	2.103	1.944	0.721	0.490	286	187.03	24.72
100	0.1	Flood	2.026	2.007	0.614	0.545	89	98.455	7.583
125	0.1	Flood	1.984	1.725	0.567	0.470	93	102.32	13.37
100	0.1	MQL	1.758	1.700	0.45	0.446	171	170.84	1.37
125	0.1	MQL	1.788	1.644	0.472	0.484	175	192.08	6.82
75	0.1	MQL+Cryo	0.959	0.918	0.417	0.415	45	45.08	1.59
100	0.1	MQL+Cryo	0.853	0.885	0.432	0.421	48	45.62	3.71
150	0.1	MQL+Cryo	0.762	0.631	0.473	0.465	52	50.95	6.89

Table 4 shows that the proposed ANN model can be adapted to the problem of interest with high accuracy. It was reported that the proposed ANN model offers the best performance in surface roughness estimation. The mean relative error for the surface roughness was obtained as 6.08%. The relative errors of the estimates for flank wear and cutting temperature were 12.38% and 8.32%, respectively. Figure 13 shows the experimental findings of surface roughness in four different environments and the estimation results made by the proposed model. It was determined that the ANN model provides the highest performance for the Dry environment in terms of surface roughness estimation in milling operations applied in different environmental conditions. It was reported that the estimation results for this environment present a mean relative error of 3.49%. For Flood, MQL and MQL+Cryo environments, the relative error performances were obtained as 6.99%, 5.64%, and 8.36%, respectively. It was observed that the proposed ANN structure for the MQL+Cryo environment can be adapted to the problem with the lowest efficiency.
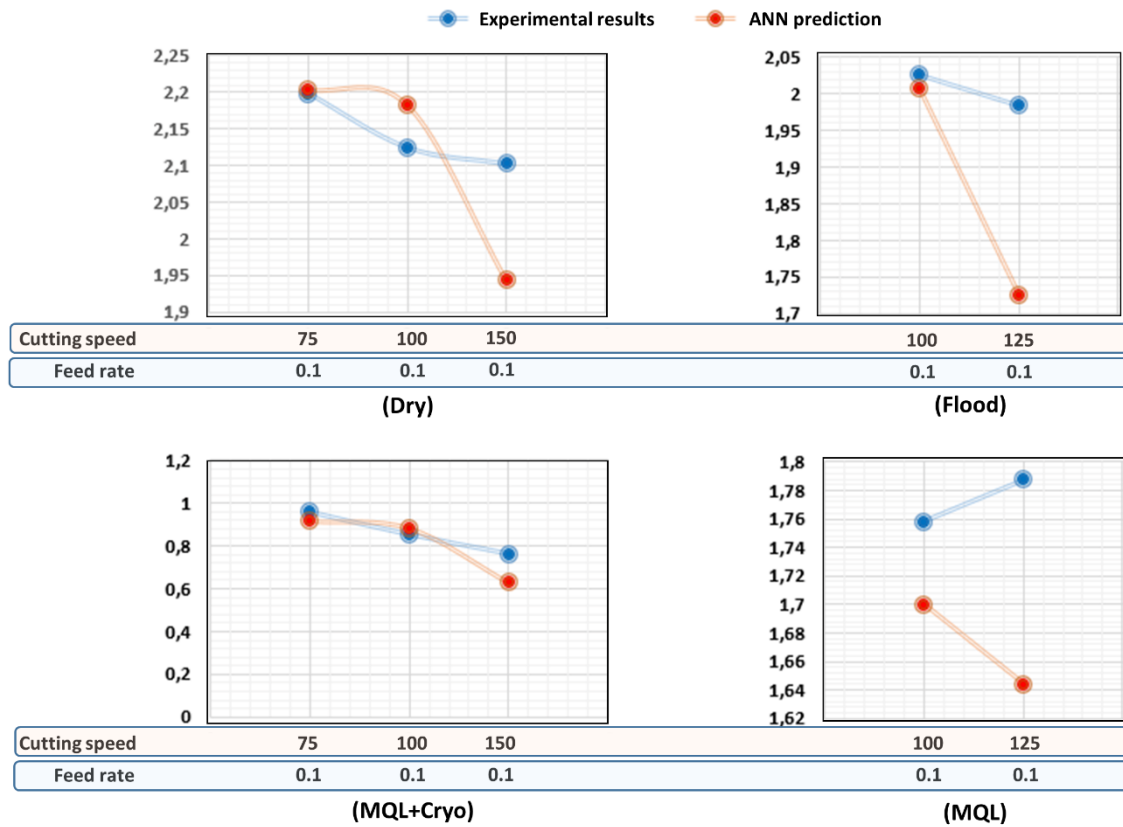
Figure 13. Comparison of experimental result and ANN prediction performance for surface roughness. Blue color represents experimental results; red represents the prediction

Figure 14 shows the experimental findings of flank wear in four different environments and the estimation results made by the proposed model. It was observed that the proposed model for flank wear could be adapted to provide results close to the experimental test findings in different ambient conditions, cutting speeds, and feed rates. It was observed that the model proposed in Figure 15 provides the most efficient predictive performance of flank wear for the MQL+Cryo environment. It was reported that the ANN model for the MQL+Cryo environment has a relative error of 1.46%. It was reported that the proposed ANN model for flank wear estimation presents an average relative error of 1.74% in the MQL environment. It was observed that the developed ANN model works in the Dry environment with the lowest efficiency and offers a relative error of 29.27% for the said environment. It was emphasized by the findings that the experimental real findings and the computer-based synthetic outputs

diverge from each other in the DRY environment. It can be said that the proposed model makes more accurate predictions for the flank wear parameter, especially for the MQL and MQL+CRYO environments, and it is more reliable for these environments.
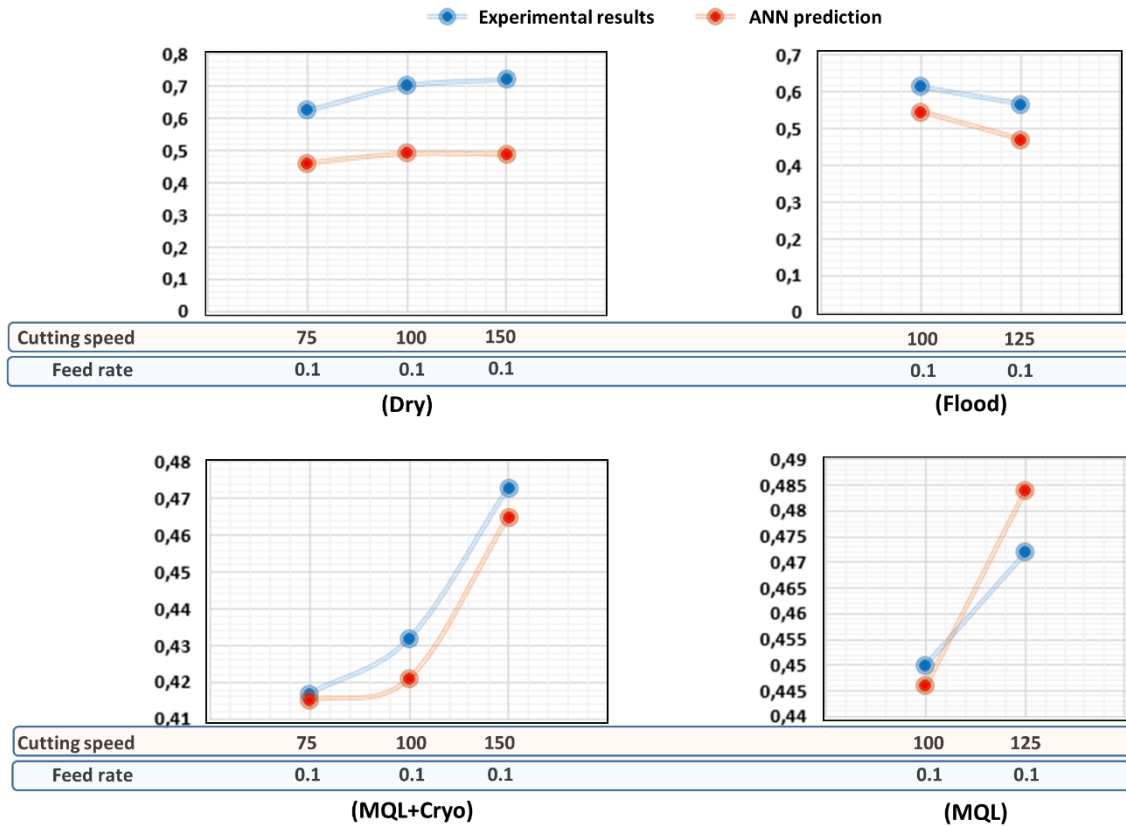

Figure 14. Comparison of experimental result and ANN prediction performance for flank wear. Blue color represents experimental results; red represents the prediction.

Figure 15 shows the experimental findings regarding the cutting temperature in four different environments and the estimation results made by the proposed model.
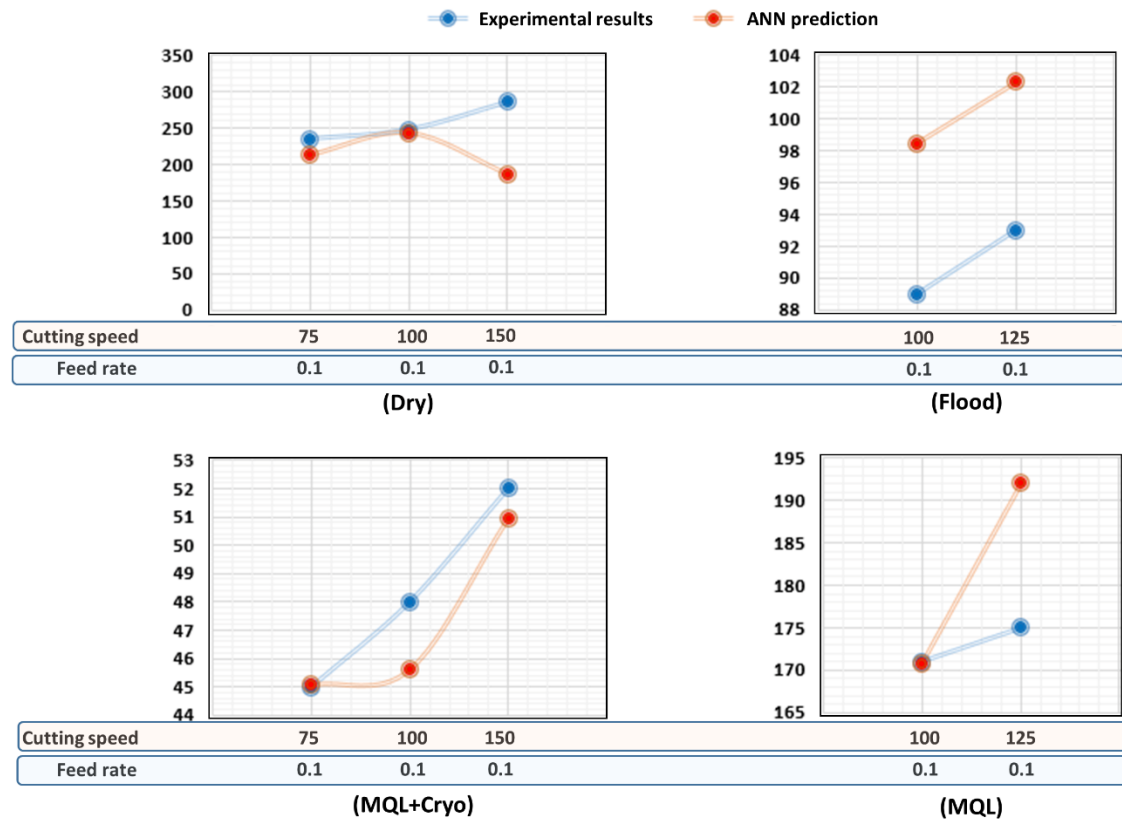
Figure 15. Comparison of experimental results and ANN prediction performance for cutting temperature. Blue color represents experimental results; red represents the prediction.

In the estimations made by the proposed ANN model for the cut-off temperature, it was reported that the effect of ambient conditions on performance is higher than other parameters. It was observed that the estimations are performed with the highest efficiency for the MQL+Cryo environment. The mean relative error for the MQL+Cryo environment was 2.38%. It was observed that the proposed model for the cutting temperature performs at a low level of efficiency in the Dry environment. The proposed ANN model showed the lowest performance for the Dry environment, presenting an average relative error of 15.19%. The high variation of the experimental findings according to the input parameters in the Dry environment can be shown as the main reason for the low performance. High variation can be considered one of the biggest obstacles to a healthy adaptation.

3.6. PSO-based optimization

This study applied the PSO technique to optimize the input parameters with the ANN model adapted to the problem. In this context, it is aimed to determine the most efficient input parameters in terms of flank wear, surface roughness, and cutting temperature factors before real-time application.

In the PSO optimizer run, the selected particles are limited to 0 to 200 for the cutting speed and between 0.00 and 0.50 for the feed rate. Thus, the particles were enabled to make observations in the relevant range. In addition, particles are limited to four different conditions for environmental conditions. Initially, 20 particles were used for each input parameter. It is aimed to predict the optimum outputs by presenting each particle to the pre-trained ANN input. At the end of 284 iterations, it was reported that 20 selected particles for each input reached the optimum value.
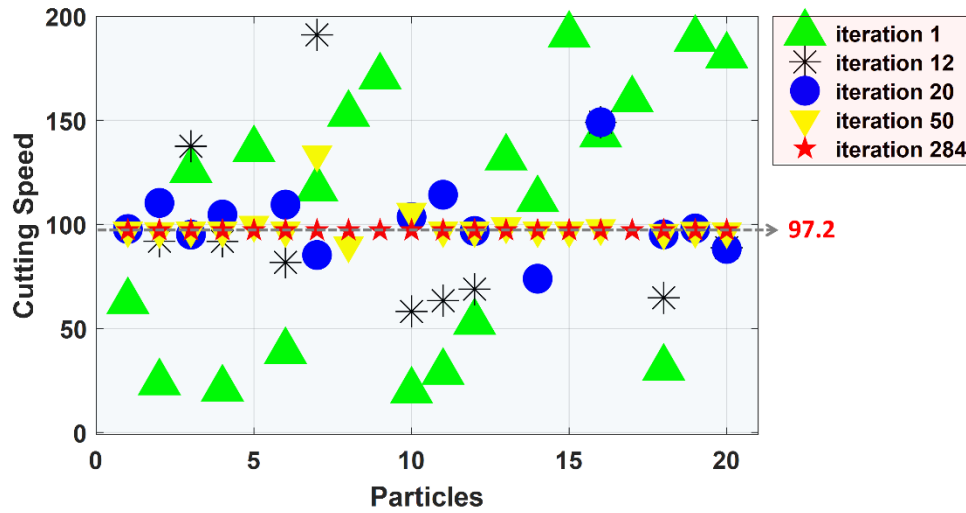

Figure 16. Sample PSO particle positions for cutting speed optimization, including 1st, 12th, 20th, 50th, and final iterations

With the proposed model, optimum cutting speed and feed rate values were determined as 97.2 and 0.0829, respectively. The PSO model also determined the MQL+Cryo environment as the optimum environmental condition. Figures 16 and 17 illustrate the trajectory of particles within the solution space as they converge towards the optimal solution for the input parameters of cutting speed and feed rate,

respectively. First, their random positions within certain limits are shown, followed by their positions in the 12th, 20th, 50th, and 284th iterations.
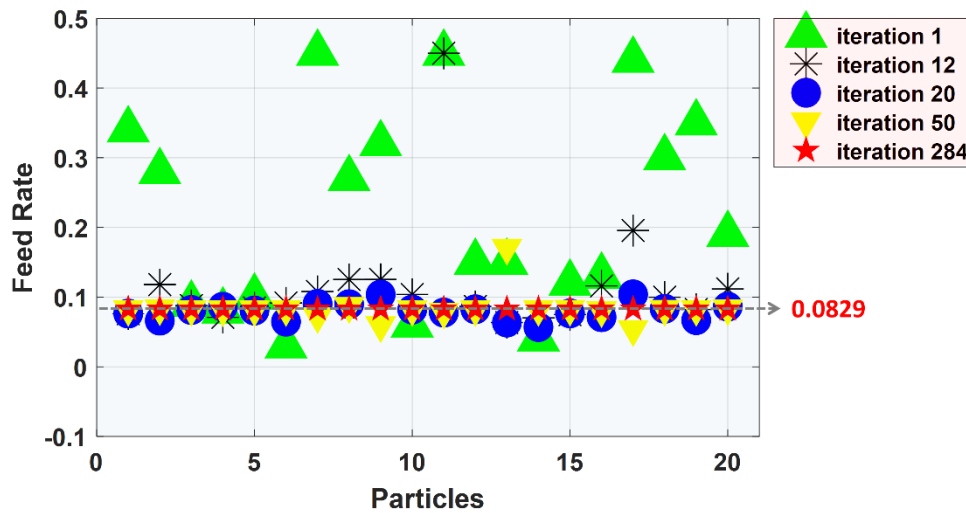

Figure 17. Sample PSO particle positions for feed rate optimization, including 1st, 12th, 20th, 50th, and final iterations

4. Conclusions

In this study, the effect of milling of Inconel 800 material in different cutting parameters and different C/L environments on machinability metrics was investigated. In addition, modeling and optimizing the relationship between outputs such as surface roughness, flank wear, and cutting temperature corresponding to the input parameters in milling nickel-based superalloys was carried out. In this context, a conventional ANN architecture was proposed during the modeling phase. The main findings can be summarized as follows;

- When milling Incoloy 800 material at high speeds, the surface roughness quality increases by approximately 30%. This effect was achieved with the sustainable MQL+Cryo C/L environment.

- For optimum flank wear values, it was seen that it would be more appropriate to choose C/L media according to cutting speed and feed rates. For example, for low shear parameters (Vc:75 m/min and fn: 0.075 mm/rev) MQL+Cryo C/L

environment plays an active role, while for high shear parameters (Vc:150 m/min and fn: 0.15 mm/rev) flood C/L environment can play an active role.

- Thanks to the excellent lubrication/cooling capability of MQL +Cryo condition, it was determined by SEM analysis that the mechanical abrasions that occur in the cutting tool are minimized.

- It shows that the proposed ANN model can be adapted to the problem of interest with high accuracy. Relative errors of 6.08%, 12.38%, and 8.32% were obtained for surface roughness, flank wear, and cutting temperature, respectively.

- It was determined that the proposed ANN model effectively estimates machinability metrics in the MQL+Cryo C/L environment. Relative errors of 8.36%, 1.46%, and 2.38% were obtained for surface roughness, flank wear, and cutting temperature, respectively.

- In the study, PSO optimization technique was applied to obtain optimum machinability metrics for the milling of Incoloy 800 material. The proposed model determined the optimum cutting speed and feed rate as 97.2 and 0.0829, respectively. The PSO model also decided the MQL+Cryo environment as the optimum environmental condition.

Statements and Declarations

Statement of originality

The submitted manuscript is ORIGINAL and the author's exclusive property(s). It has not been published, nor have substantial portions of the work been published, nor is it under consideration for publication in another journal.

Declaration of Competing Interest

The author(s) affirm that there are no conceivable conflicts of interest pertaining to the research, composition, and publication of this article.

Acknowledgements

Data Availability Statement

Data sharing is not applicable to this article as no datasets were generated or analysed during the current study.

Author Contributions

All authors actively participated in formulating and designing the study. [Emine Şap], [Üsame Ali Usca], [Serhat Şap], [Khaled Giasin], [Hasan Polat], and [Mete Kalyoncu] were responsible for material preparation, data collection, and analysis. The initial draft of the manuscript was authored by [Emine Şap], with all authors contributing to subsequent revisions. The final version of the manuscript was reviewed, approved, and endorsed by all authors.

References

[1] C. Sinu, S. Veena, H. Subramanian, S. Bera, P.K. Aji Kumar, P. Chandramohan, T. Mathews, T.V. Krishna Mohan, Interaction of magnesium ions in high temperature aqueous solution with Incoloy-800, Mater. Today Commun., 33 (2022) 104454.doi: https://doi.org/10.1016/j.mtcomm.2022.104454

[2] S. Rubaiee, M. Danish, M.K. Gupta, A. Ahmed, S.M. Yahya, M.B. Yildirim, M. Sarikaya, M.E. Korkmaz, Key initiatives to improve the machining characteristics of Inconel-718 alloy: Experimental analysis and optimization, J. Mater. Res. Technol., 21 (2022) 2704-2720.doi: https://doi.org/10.1016/j.jmrt.2022.10.060

[3] J. Zhao, Z. Liu, B. Wang, Y. Hua, Q. Wang, Cutting temperature measurement using an improved two-color infrared thermometer in turning Inconel 718 with whisker-reinforced ceramic tools, Ceram. Int., 44 (2018) 19002-19007.doi: https://doi.org/10.1016/j.ceramint.2018.07.142

[4] M.E. Korkmaz, M.K. Gupta, M. Boy, N. Yaşar, G.M. Krolczyk, M. Günay, Influence of duplex jets MQL and nano-MQL cooling system on machining performance of Nimonic 80A, Manuf. Process, 69 (2021) 112-124.doi: https://doi.org/10.1016/j.jmapro.2021.07.039

[5] Ç.V. Yıldırım, M. Sarıkaya, T. Kıvak, Ş. Şirin, The effect of addition of hBN nanoparticles to nanofluid-MQL on tool wear patterns, tool life, roughness and temperature in turning of Ni-based Inconel 625, Tribol. Int., 134 (2019) 443-456.doi: https://doi.org/10.1016/j.triboint.2019.02.027

[6] X. Cui, B. Zhao, F. Jiao, J. Zheng, Chip formation and its effects on cutting force, tool temperature, tool stress, and cutting edge wear in high- and ultra-high-speed milling, Int. J. Adv. Manuf. Technol., 83 (2016) 55-65.doi: 10.1007/s00170-015-7539-7

[7] E. Salur, M. Kuntoğlu, A. Aslan, D.Y. Pimenov, The Effects of MQL and Dry Environments on Tool Wear, Cutting Temperature, and Power Consumption during End Milling of AISI 1040 Steel, Metals, 2021.

[8] E. Salur, Understandings the tribological mechanism of Inconel 718 alloy machined under different cooling/lubrication conditions, Tribol. Int., 174 (2022) 107677.doi: https://doi.org/10.1016/j.triboint.2022.107677

[9] E. Şap, Ü.A. Usca, M. Uzun, Machining and optimization of reinforced copper composites using different cooling-lubrication conditions, J. Braz. Soc. Mech. Sci. & Eng., 44 (2022) 399.doi: 10.1007/s40430-022-03678-6

[10] Ü.A. Usca, M. Uzun, S. Şap, K. Giasin, D.Y. Pimenov, C. Prakash, Determination of machinability metrics of AISI 5140 steel for gear manufacturing using different cooling/lubrication conditions, J. Mater. Res. Technol., 21 (2022) 893-904.doi: https://doi.org/10.1016/j.jmrt.2022.09.067

[11] R. Binali, H. Demirpolat, M. Kuntoglu, H. Saglam, Machinability Investigations Based on Tool Wear, Surface Roughness, Cutting Temperature, Chip Morphology and Material Removal Rate during Dry and MQL-Assisted Milling of Nimax Mold Steel, Lubricants, 11 (2023).doi: ARTN 101

10.3390/lubricants11030101

[12] R. Binali, H. Demirpolat, M. Kuntoglu, E. Salur, Different Aspects of Machinability in Turning of AISI 304 Stainless Steel: A Sustainable Approach with MQL Technology, Metals, 13 (2023).doi: ARTN 1088

10.3390/met13061088

[13] M. Hemmat Esfe, M. Bahiraei, A. Mir, Application of conventional and hybrid nanofluids in different machining processes: A critical review, Adv Colloid Interface Sci, 282 (2020) 102199.doi: https://doi.org/10.1016/j.cis.2020.102199

[14] H. Demirpolat, R. Binali, A.D. Patange, S.S. Pardeshi, S. Gnanasekaran, Comparison of Tool Wear, Surface Roughness, Cutting Forces, Tool Tip Temperature,

and Chip Shape during Sustainable Turning of Bearing Steel, Materials, 16 (2023).doi: ARTN 4408

10.3390/ma16124408

[15] Ü.A. Usca, The Effect of Cellulose Nanocrystal-Based Nanofluid on Milling Performance: An Investigation of Dillimax 690T, Polymers, 15 (2023) 4521

[16] O. Pereira, A. Rodríguez, A.I. Fernández-Abia, J. Barreiro, L.N. López de Lacalle, Cryogenic and minimum quantity lubrication for an eco-efficiency turning of AISI 304, J. Clean. Prod., 139 (2016) 440-449.doi: https://doi.org/10.1016/j.jclepro.2016.08.030

[17] N.S. Ross, M. Ganesh, D. Srinivasan, M.K. Gupta, M.E. Korkmaz, J.B. Krolczyk, Role of sustainable cooling/lubrication conditions in improving the tribological and machining characteristics of Monel-400 alloy, Tribol. Int., 176 (2022) 107880.doi: https://doi.org/10.1016/j.triboint.2022.107880

[18] N. Khanna, P. Shah, R.W. Maruda, G.M. Krolczyk, H. Hegab, Experimental investigation and sustainability assessment to evaluate environmentally clean machining of 15-5 PH stainless steel, Manuf. Process, 56 (2020) 1027-1038.doi: https://doi.org/10.1016/j.jmapro.2020.05.016

[19] Ü. Değirmenci, Ü.A. Usca, S. Şap, Machining characterization and optimization under different cooling/lubrication conditions of Al-4Gr hybrid composites fabricated by vacuum sintering, Vacuum, 208 (2023) 111741.doi: https://doi.org/10.1016/j.vacuum.2022.111741

[20] B. Tasdelen, T. Wikblom, S. Ekered, Studies on minimum quantity lubrication (MQL) and air cooling at drilling, J. Mater. Process. Technol., 200 (2008) 339-346.doi: https://doi.org/10.1016/j.jmatprotec.2007.09.064

[21] A.M. Khan, M. Jamil, M. Mia, D.Y. Pimenov, V.R. Gasiyarov, M.K. Gupta, N. He, Multi-Objective Optimization for Grinding of AISI D2 Steel with Al2O3 Wheel under MQL, Materials, 2018.

[22] M.A. Sampaio, Á.R. Machado, C.A.H. Laurindo, R.D. Torres, F.L. Amorim, Influence of minimum quantity of lubrication (MQL) when turning hardened SAE 1045 steel: a comparison with dry machining, Int. J. Adv. Manuf. Technol., 98 (2018) 959-968.doi: 10.1007/s00170-018-2342-x

[23] S. Şap, Ü.A. Usca, Y.S. Tarih, A. Yar, M. Kuntoğlu, M.K. Gupta, Novel Use of Cellulose Based Biodegradable Nano Crystals in the Machining of PPS Composites: An Approach Towards Green Machining, Int. J. Precis. Eng. Manuf., 11 (2024) 1-19.doi: 10.1007/s40684-023-00529-0

[24] Q. Yin, C. Li, Y. Zhang, M. Yang, D. Jia, Y. Hou, R. Li, L. Dong, Spectral analysis and power spectral density evaluation in Al2O3 nanofluid minimum quantity lubrication milling of 45 steel, Int. J. Adv. Manuf. Technol., 97 (2018) 129-145.doi: 10.1007/s00170-018-1942-9

[25] Chetan, S. Ghosh, P.V. Rao, Comparison between sustainable cryogenic techniques and nano-MQL cooling mode in turning of nickel-based alloy, J. Clean. Prod., 231 (2019) 1036-1049.doi: https://doi.org/10.1016/j.jclepro.2019.05.196

[26] Y.V. Deshpande, A.B. Andhare, P.M. Padole, How cryogenic techniques help in machining of nickel alloys? A review, Mach. Sci. Technol., 22 (2018) 543-584.doi: 10.1080/10910344.2017.1382512

[27] Ç.V. Yıldırım, T. Kıvak, M. Sarıkaya, Ş. Şirin, Evaluation of tool wear, surface roughness/topography and chip morphology when machining of Ni-based alloy 625 under MQL, cryogenic cooling and CryoMQL, J. Mater. Res. Technol., 9 (2020) 2079-2092.doi: https://doi.org/10.1016/j.jmrt.2019.12.069

[28] N. Khanna, C. Agrawal, M.K. Gupta, Q. Song, Tool wear and hole quality evaluation in cryogenic Drilling of Inconel 718 superalloy, Tribol. Int., 143 (2020) 106084.doi: https://doi.org/10.1016/j.triboint.2019.106084

[29] Ç.V. Yıldırım, Investigation of hard turning performance of eco-friendly cooling strategies: Cryogenic cooling and nanofluid based MQL, Tribol. Int., 144 (2020) 106127.doi: https://doi.org/10.1016/j.triboint.2019.106127

[30] J. Chen, W. Yu, Z. Zuo, Y. Li, D. Chen, Q. An, H. Wang, M. Chen, Tribological properties and tool wear in milling of in-situ TiB2/7075 Al composite under various cryogenic MQL conditions, Tribol. Int., 160 (2021) 107021.doi: https://doi.org/10.1016/j.triboint.2021.107021

[31] M.K. Gupta, M. Mia, M. Jamil, R. Singh, A.K. Singla, Q. Song, Z. Liu, A.M. Khan, M.A. Rahman, M. Sarikaya, Machinability investigations of hardened steel with biodegradable oil-based MQL spray system, Int. J. Adv. Manuf. Technol., 108 (2020) 735-748.doi: 10.1007/s00170-020-05477-6

[32] S. Min, I. Inasaki, S. Fujimura, T. Wada, S. Suda, T. Wakabayashi, A Study on Tribology in Minimal Quantity Lubrication Cutting, CIRP Annals, 54 (2005) 105-108.doi: https://doi.org/10.1016/S0007-8506(07)60060-2

[33] S. Şap, M. Uzun, Ü.A. Usca, D.Y. Pimenov, K. Giasin, S. Wojciechowski, Investigation of machinability of Ti–B-SiCp reinforced Cu hybrid composites in dry turning, J. Mater. Res. Technol., 18 (2022) 1474-1487.doi: https://doi.org/10.1016/j.jmrt.2022.03.049

[34] S. Haykin, Neural networks and learning machines, 3/E, Pearson Education India2009.

[35] D.S. Pandey, S. Das, I. Pan, J.J. Leahy, W. Kwapinski, Artificial neural network based modelling approach for municipal solid waste gasification in a fluidized bed reactor, Waste Manage., 58 (2016) 202-213.doi: https://doi.org/10.1016/j.wasman.2016.08.023

[36] M. Arafat, T. Sjafrizal, R.A. Anugraha, An artificial neural network approach to predict energy consumption and surface roughness of a natural material, SN App. Sci., 2 (2020) 1174.doi: 10.1007/s42452-020-2987-6

[37] S. Dreiseitl, L. Ohno-Machado, Logistic regression and artificial neural network classification models: a methodology review, J Biomed. Inform., 35 (2002) 352-359.doi: https://doi.org/10.1016/S1532-0464(03)00034-0

[38] Ş. Karabulut, Optimization of surface roughness and cutting force during AA7039/Al2O3 metal matrix composites milling using neural networks and Taguchi method, Measurement, 66 (2015) 139-149.doi: https://doi.org/10.1016/j.measurement.2015.01.027

[39] U. Maheshwera Reddy Paturi, H. Devarasetti, S. Kumar Reddy Narala, Application Of Regression And Artificial Neural Network Analysis In Modelling Of Surface Roughness In Hard Turning Of AISI 52100 Steel, Mater. Today: Proc., 5 (2018) 4766-4777.doi: https://doi.org/10.1016/j.matpr.2017.12.050

[40] M. Yanis, A. Mohruni, S. Sharif, I. Yani, A. Arifin, B. Khona'Ah, Application of RSM and ANN in predicting surface roughness for side milling process under environmentally friendly cutting fluid, Journal of Physics: Conference Series, IOP Publishing, 2019, pp. 042016.

[41] S. Bharathi Raja, N. Baskar, Optimization techniques for machining operations: a retrospective research based on various mathematical models, Int. J. Adv. Manuf. Technol., 48 (2010) 1075-1090.doi: 10.1007/s00170-009-2351-x

[42] S.O. Fadlallah, T.N. Anderson, R.J. Nates, Artificial Neural Network–Particle Swarm Optimization (ANN-PSO) Approach for Behaviour Prediction and Structural Optimization of Lightweight Sandwich Composite Heliostats, Arab. J. Sc.i Eng., 46 (2021) 12721-12742.doi: 10.1007/s13369-021-06126-0

[43] D.E. Goldberg, Genetic Algorithms in Search, Optimization and Machine Learning, Addison Wesley Longman Publishing Co., New York, USA, 1989.

[44] J. Kennedy, R. Eberhart, Particle swarm optimization, Proceedings of ICNN'95-international conference on neural networks, IEEE, 1995, pp. 1942-1948.

[45] M. Dorigo, G. Di Caro, Ant colony optimization: a new meta-heuristic, Proceedings of the 1999 congress on evolutionary computation-CEC99 (Cat. No. 99TH8406), IEEE, 1999, pp. 1470-1477.

[46] D. Karaboga, B. Akay, Artificial bee colony (ABC) algorithm on training artificial neural networks, 2007 IEEE 15th Signal Processing and Communications Applications, IEEE, 2007, pp. 1-4.

[47] M. Azab, Global maximum power point tracking for partially shaded PV arrays using particle swarm optimisation, Int. J. Renew. Energy Res., 1 (2009) 211-235

[48] R. Venkata Rao, P.J. Pawar, Parameter optimization of a multi-pass milling process using non-traditional optimization algorithms, Appl. Soft Comput., 10 (2010) 445-456.doi: https://doi.org/10.1016/j.asoc.2009.08.007

[49] W.-a. Yang, Y. Guo, W.-h. Liao, Optimization of multi-pass face milling using a fuzzy particle swarm optimization algorithm, Int. J. Adv. Manuf. Technol., 54 (2011) 45-57.doi: 10.1007/s00170-010-2927-5

[50] M. Farahnakian, M.R. Razfar, M. Moghri, M. Asadnia, The selection of milling parameters by the PSO-based neural network modeling method, Int. J. Adv. Manuf. Technol., 57 (2011) 49-60.doi: 10.1007/s00170-011-3262-1

[51] N. Yusup, A.M. Zain, S.Z.M. Hashim, Overview of PSO for Optimizing Process Parameters of Machining, Procedia Eng., 29 (2012) 914-923.doi: https://doi.org/10.1016/j.proeng.2012.01.064

[52] M. Chandrasekaran, S. Tamang, ANN–PSO Integrated Optimization Methodology for Intelligent Control of MMC Machining, J. Inst. Eng. (India): C, 98 (2017) 395-401.doi: 10.1007/s40032-016-0276-3

[53] R. Dehmolaei, M. Shamanian, A. Kermanpur, Microstructural characterization of dissimilar welds between alloy 800 and HP heat-resistant steel, Mater Charact, 59 (2008) 1447-1454.doi: 10.1016/j.matchar.2008.01.013

[54] P. Karmiris-Obratański, N.E. Karkalos, R. Kudelski, A.P. Markopoulos, Experimental study on the effect of the cooling method on surface topography and workpiece integrity during trochoidal end milling of Incoloy 800, Tribol. Int., 176 (2022) 107899.doi: https://doi.org/10.1016/j.triboint.2022.107899

[55] V. Mundada, S. Kumar Reddy Narala, Optimization of Milling Operations Using Artificial Neural Networks (ANN) and Simulated Annealing Algorithm (SAA), Mater. Today: Proc., 5 (2018) 4971-4985.doi: https://doi.org/10.1016/j.matpr.2017.12.075

[56] P. Umapathy, C. Venkataseshaiah, M.S. Arumugam, Particle Swarm Optimization with Various Inertia Weight Variants for Optimal Power Flow Solution, Discrete Dyn Nat Soc, 2010 (2010) 462145.doi: 10.1155/2010/462145

[57] N. Khanna, J. Airao, G. Kshitij, C.K. Nirala, H. Hegab, Sustainability analysis of new hybrid cooling/lubrication strategies during machining Ti6Al4V and Inconel 718 alloys, SM&T, 36 (2023) e00606.doi: https://doi.org/10.1016/j.susmat.2023.e00606

[58] M.N. Babu, V. Anandan, Ç.V. Yıldırım, M.D. Babu, M. Sarıkaya, Investigation of the characteristic properties of graphene-based nanofluid and its effect on the turning performance of Hastelloy C276 alloy, Wear, 510-511 (2022) 204495.doi: https://doi.org/10.1016/j.wear.2022.204495

[59] D. Umbrello, Investigation of surface integrity in dry machining of Inconel 718, The International Journal of Advanced Manufacturing Technology, 69 (2013) 2183-2190.doi: 10.1007/s00170-013-5198-0

[60] A. Thakur, S. Gangopadhyay, State-of-the-art in surface integrity in machining of nickel-based super alloys, International Journal of Machine Tools and Manufacture, 100 (2016) 25-54.doi: https://doi.org/10.1016/j.ijmachtools.2015.10.001

[61] R.B. da Silva, Á.R. Machado, E.O. Ezugwu, J. Bonney, W.F. Sales, Tool life and wear mechanisms in high speed machining of Ti–6Al–4V alloy with PCD tools under various coolant pressures, J. Mater. Process. Technol., 213 (2013) 1459-1464.doi: https://doi.org/10.1016/j.jmatprotec.2013.03.008

[62] N. Tamil Alagan, P. Hoier, P. Zeman, U. Klement, T. Beno, A. Wretland, Effects of high-pressure cooling in the flank and rake faces of WC tool on the tool wear mechanism and process conditions in turning of alloy 718, Wear, 434-435 (2019) 102922.doi: https://doi.org/10.1016/j.wear.2019.05.037

[63] S. Şap, Understanding the Machinability and Energy Consumption of Al-Based Hybrid Composites under Sustainable Conditions, Lubricants, 11 (2023) 111.doi: https://doi.org/10.3390/lubricants11030111

[64] Ü.A. Usca, S. Şap, M. Uzun, Evaluation of Machinability of Cu Matrix Composite Materials by Computer Numerical Control Milling under Cryogenic LN2 and Minimum Quantity Lubrication, J. Mater. Eng. Perform., 32 (2023) 2417-2431.doi: https://doi.org/10.1007/s11665-022-07262-w